# Symmetric interaction of developing horizontal jet in a stratified fluid with a vertical cylinder

S. I. Voropayev and Ya. D. Afanasyev
*Institute of Oceanology, Russian Academy of Sciences, Moscow 117218, Russia*

(Received 26 January 1993; accepted 11 January 1994)

A self-similar planar vortex dipole, arising at the front of developing horizontal jet in a stratified fluid, collides with a small vertical cylinder. The primary vortical flow interacts with the secondary vorticity generated at the boundary of the cylinder and finally a new dipole of reduced intensity forms. The estimates for the reduction of the flow momentum and alteration of the overall propagation velocity and length scales of the newly formed dipole are given. The evolution of the real flow is also explained mathematically.

## I. INTRODUCTION

The problem of interaction of compact vortex structures with solid bodies is of central importance for various technical and geophysical applications. Stern and Whitehead[1] have considered the separation of a near-wall jet in a rotating fluid in the laboratory experiment and numerically using a contour dynamics method. The separation of the impulsive vortex dipole, which moves along a vertical wall in a stratified fluid, was observed by Voropayev and Afanasyev.[2] In the latter case, the combined effects of image vortices and the secondary vorticity produced at the wall cause the rebound of the primary vortex structure from the wall. The eruption of the dipole from the wall resembles the bursting phenomena in the near-wall region of the turbulent boundary layer (Falco[3] and Robinson[4]).

A dipolar vortical flow impinging normally on a vertical barrier in a stratified fluid was reproduced by van Heijst and Flor.[5] Using this experiment as a basis, Orlandi[6] made two-dimensional numerical simulations of the collision. Nonslip and free-slip boundary conditions were considered. The simulations with the nonslip conditions have demonstrated a convincing agreement with the experiment for moderate Reynolds numbers. For large Reynolds numbers, the simulations have shown a rather complex sequence of multiple rebounds and impingement's of vortex structure at the intermediate stage of collision. These effects are due to the creation of secondary and even tertiary vorticity at the wall by the primary flow. Thus the viscosity plays the crucial role in these interactions.

Homa *et al.*[7] have studied experimentally the interaction of two-dimensional vortex dipoles with small bodies: cylinders and plates. They have found that central to the process of interaction is the generation of secondary vortices of opposite sense relative to those of the corresponding primary vortices.

In general, the interaction dynamics of a dipole with a solid body closely resembles the collision of two dipoles of different intensities. In qualitative experiments in Ref. 2 it is shown that for the case of symmetric collision of two dipoles of different momenta, say $I$ and $I_0 (I > I_0)$, the final result of the interaction is a new single dipole of reduced intensity $I_* = I - I_0$. One can expect that for the case of a symmetric collision of a dipole with a small solid body the final result of interaction will be similar. To verify this prediction, we have reproduced, in a qualitative experiment, the central collision of the impulsive planar dipole, generated in a stratified fluid, with a small vertical cylinder. As one can see in Fig. 1, after the intermediate stage [Figs. 1(b) and 1(c)] a new single dipole of reduced intensity finally forms [Figs. 1(d) and 1(e)] and moves in the same direction as a primary dipole. Homa *et al.*[7] have studied experimentally and described in detail only the intermediate stage of symmetric collision of a dipole with a small cylinder. The final stage of interaction—the formation of a single dipolar structure of reduced intensity, was not studied previously.

The similarity between the interaction of a dipole with a small body and a collision of two dipoles of different momenta is obvious (compare Fig. 1 in present paper and Fig. 10 in Ref. 2) and it has a simple physical ground. Because of the non-slip conditions at the boundary of the solid body, the primary flow acts on a body with some force, hence, the body acts on the ambient fluid with the opposite force. When the body is small, this force can be considered as a localized one. The action of a localized force on a viscous fluid with the necessity gives rise to the formation of the secondary dipolar flow (see Cantwell[8] and Voropayev and Afanasyev[2]) directed against the primary flow. Thus, to explain qualitatively the interaction with a solid body, one can use the same arguments which were used in Ref. 2 to explain the collision of two dipoles of different momenta. The intensity $I_0$ of the secondary dipolar flow, induced by a solid body, is a complicated function of time, position, and geometry of the body and the intensity $I$ of the primary flow. The main aim of the present study is to estimate this function for the primary dipolar flow with controllable characteristics and intensity $I$ and, hence. to calculate the reduced intensity $I_* = I - I_0$ of the newly formed dipolar flow. The calculated values of $I_*$ then are compared with those obtained in the experiments. For this purpose, a simple experimental geometry is used. The primary flow represents a self-similar planar vortex dipole, arising at the front of a developing horizontal round jet in a density stratified fluid. The body is a small vertical cylinder placed at the axis of the flow. The intensity of the primary flow is easily controlled in the experiments and the main characteristics of these flows are well documented previously.[9]

In conjunction with the experimental data and some es-

 1070-6631/94/6(6)/2032/6/$6.00 

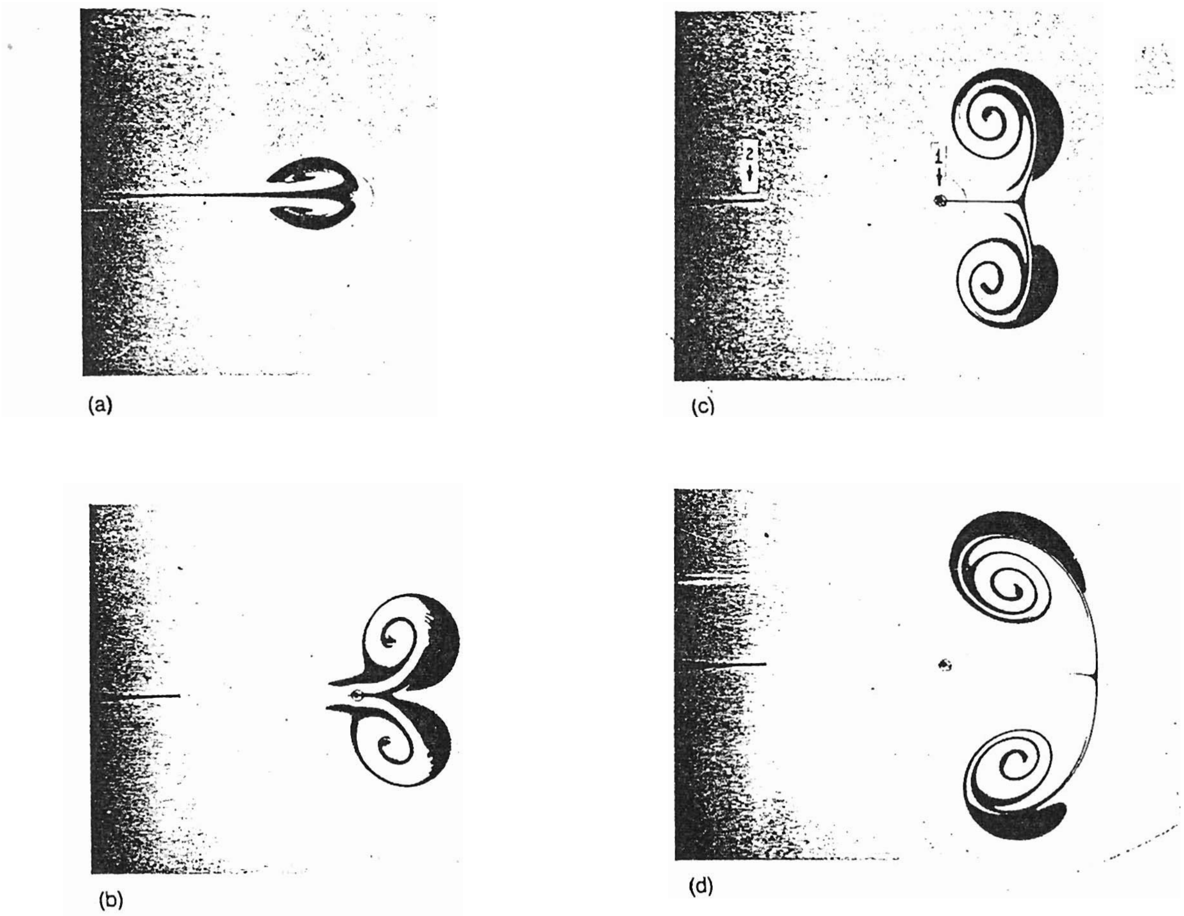


FIG. 1. Sequence of plan view photographs showing the central collision of the impulsive planar vortex dipole, generated in a linearly stratified fluid, with a small vertical cylinder (1). A single dipole, which is a final result of interaction, is clearly seen in the last two photographs. The primary dipolar flow was generated by the jet from a small round nozzle (2). The source acts for a time period $\Delta t=5$ s and transports to the fluid the impulse $I=J\Delta t=0.12\ \mathrm{cm}^4\ \mathrm{s}^{-1}$, where $J$ is a momentum flux (divided by the density) from the nozzle. The diameter of the cylinder $2a=0.125$ cm, the distance of the cylinder from the nozzle $\delta=4.4$ cm and the buoyancy frequency $N=2\ \mathrm{s}^{-1}$. The photographs were taken at (a) $t=2$, (b) 9, (c) 17, and (d) 48 s after the forcing started. Note that the cylinder is much smaller than its supporter visible in the photographs.

timates, a mathematical two-dimensional planar model of the interaction process is also proposed.

## II. DESCRIPTION OF THE EXPERIMENT AND CHARACTERISTICS OF THE PRIMARY FLOW

The experimental technique is similar to those described in detail in Refs. 2 and 9. Here we omit the details and give only a brief description. The experiments were performed in a glass tank, $25\times40\times10$ cm, filled with a stratified fluid. The tank was lightened from the bottom by luminescent lamps. A strong stable density stratification was created by varying the salinity of distilled water in the vertical ($z$) direction. Approximately linear vertical density distribution $\rho(z)\approx\rho_0[1-(N^2z/g)]$ with buoyancy (Brunt–Väisälä) frequency $N=(-g/\rho_0)(d\rho/dz)=2\ \mathrm{s}^{-1}$ ($g$ is the acceleration due to gravity) was produced in the working tank using the two-tank method.

The primary dipolar flow was generated in the tank by a submerged horizontal jet from a thin round nozzle—localized source of momentum, nozzle diameter $d=0.07$ cm. A dyed jet of density $\rho_0$ is injected horizontally in the middle of the depth of the stratified fluid at the level of its equilibrium density $z=0$. A jet exerts on the fluid a localized force $\rho_0 J=4\rho_0 q^2/(\pi d^2)$ and imparts to the fluid the impulse given by $\rho_0 I=\int_0^t\rho_0 J\,dt$, where $q$ is a small measured volume flux from the nozzle and the dimensions of $J$ are $L^4T^{-2}$. The nondimensional intensity of the source is characterized by a nondimensional governing parameter $J/\nu^2\gg1$, which is equal to a squared Reynolds number of the flow: $J/\nu^2=\mathrm{Re}^2$ (e.g., Batchelor[10]), where $\nu$ is a kinematic viscosity. Note, that another nondimensional parameter $q/\nu$ is unessential here and does not enter the problem for large distances from the origin compared to the nozzle diameter.[9,10] For a source of constant intensity, used in the experiments, the impulse of the flow increases linearly with time $t$ from the beginning of the experiment: $\rho_0 I = \rho_0 Jt$.

Typical photographs of the flow generated by this method are shown in Fig. 2. It presents the vortex dipole with a typical spiral structure at the front of the narrow conical jet. The flows of this type are well documented: they were studied experimentally,[9] reproduced in three-dimensional numerical simulations[11] and analyzed theoretically.[12] For further analysis, the main characteristics of these dipolar flows are needed and they are summarized briefly below.

Initially, or at small distances $x$ from the origin, the flow

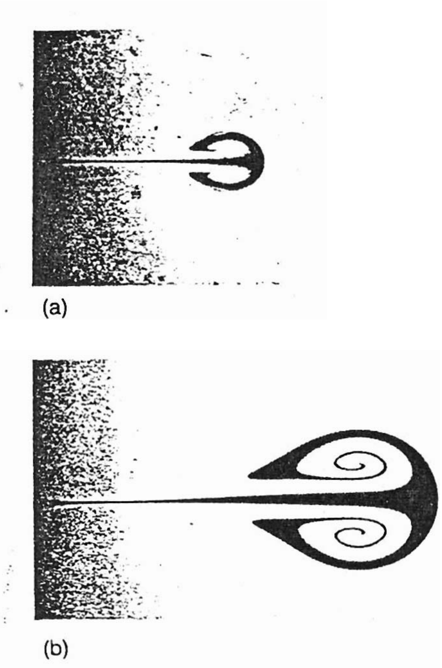


FIG. 2. Plan view photographs showing the planar dipole at the front of the developing jet in a stratified fluid. The experimental parameters are $N=2$ $s^{-1}$, $Re^2=J/\nu^2=3500$. The photographs were taken at (a) $t=3$ and (b) 21 s after the forcing started.

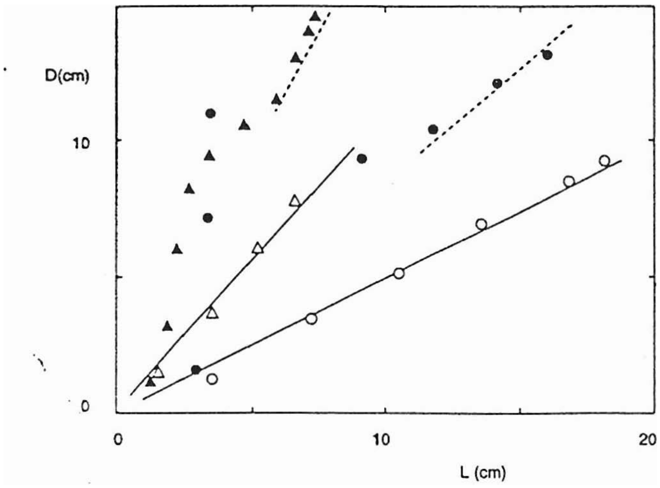


FIG. 3. Measured values of the width $D$ of the dipole for different distances $L$ from the origin to the center of the dipole ($L=L_*-D/2$, where $L_*$ is the distance to the front of the dipole) for two experiments (△,○) without a cylinder and for two experiments (▲,●) with a cylinder at the same values of $J$. The experimental parameters are $N=2$ $s^{-1}$, $Re^2=J/\nu^2=1385$ (△,▲), 6720 (○,●), $2a$, $\delta=0.125$ cm, 2 cm (▲), 0.21 cm, 4 cm (●). The solid lines through the open symbols (△,○) represent the estimate (1) with $\alpha$(Re) given by the graph in Fig. 11 in Ref. 9. The dashed lines through the solid symbols (▲,●) represent the estimate (1) for the newly formed dipole of reduced intensity $Re_*^2=J_*/\nu^2$ given by (5).

is governed by two nondimensional parameters: the Reynolds number $Re=\sqrt{J}/\nu$ and the Richardson number $Ri=\nu^4N^2x^4/(A^2BJ^3)$ [$A=3/(8\pi)$, $B=3/(64\pi)$]. As a consequence of conservation of momentum flux, the first parameter is constant along the axis of the flow ($x$ axis), while the second one increases rapidly with the distance $x$ from the origin. When $x$ exceeds some critical value $x>x_0$, which is equal to $x_0=(\nu^2A^2B\ Re^6/N^2)^{1/4}$ (in the experiments $x_0\leq 1$ cm), the conditions $Re\gg 1$, $Re\ Ri\gg 1$ become valid and the vertical component of the velocity in the flow is absent.[12] At $x>x_0$, the fluid particles move in horizonal planes and the flow is planar. At the asymptote $x\gg x_0$ the Richardson number is sufficiently large, it does not enter the problem directly and the characteristics of the planar flow are determined only by the Reynolds number. Note, that at small $Ri(x\ll x_0)$, when the influence of stratification is negligible, the flow demonstrates another behavior. The motion at that asymptote ($x\ll x_0$) is axisymmetric and resembles a spherical vortex which develops at the front of the jet in a homogeneous fluid and travels away from the origin (see photograph on the cover of Batchelor's book[10] and Figs. 1 and 2 in Ref. 9). Below, we neglect the short asymptote at $x<x_0$ and consider only the prolonged asymptote at $x>x_0$ when the motion is horizontal. The flow has no external length scale, thus it develops in a self-similar manner. The horizontal cross-width $D$ of the frontal dipole and the distance $L$ from the origin to the center of the dipole (more precisely $L=L_*-D/2$, where $L_*$ is the distance to the front of the dipole) changes with time as

$$D=\alpha L, \tag{1}$$

$$L=Re(2A\beta\nu t)^{1/2}, \tag{2}$$

while the distribution of the longitudinal velocity $V$ across the axis of the narrow conical jet, which inflows into the dipole, is given by[9,12]

$$V=\frac{A\nu\ Re^2}{x(1+B\ Re^2\ r^2/x^2)^2}, \tag{3}$$

where $r^2=y^2+z^2$, $x$, $y$, and $z$ are the longitudinal, lateral and vertical coordinates with the origin coincided with the flow origin, and the propagation velocity $\bar{V}=dL/dt$ of the dipole is proportional to $\bar{V}=\beta V(r=0,x=L)=\beta V_0$. The calculated and measured in the experiment values of the nondimensional functions $\alpha$(Re) and $\beta$(Re) can be found in graphs in Fig. 11 in Ref. 9. In the present experiments, the collision of this primary dipolar flow with a small vertical cylinder, diameter $2a=0.125$ or 0.21 cm, was studied. The cylinder was fixed at the bottom of the tank at the axis of the flow at the distance $\delta=2$ or 4 cm from the nozzle ($\delta\gg x_0$). The source of motion was turned on when all motions in the tank were practically absent. The information about the flow evolution was obtained photographically. For the flow visualization, the pH-indicator thymol blue was used.[2,9]

## III. EXPERIMENTAL RESULTS AND INTERPRETATION

In the first series of the experiments, the primary flow without a cylinder was reproduced. A typical example of the flow is shown in Fig. 2. The measured values of $D$ and $L$ are shown by the open symbols in Figs. 3 and 4 for two experiments with different values of $J$. To compare the measured values of $D$ and $L$ with the estimates given by (1) and (2), the graphs in Fig. 11 in Ref. 9 were used. By means of these graphs, the values of $\alpha$ and $\beta$ for each value of $J$ were determined and the resulting estimates (1) and (2) are shown

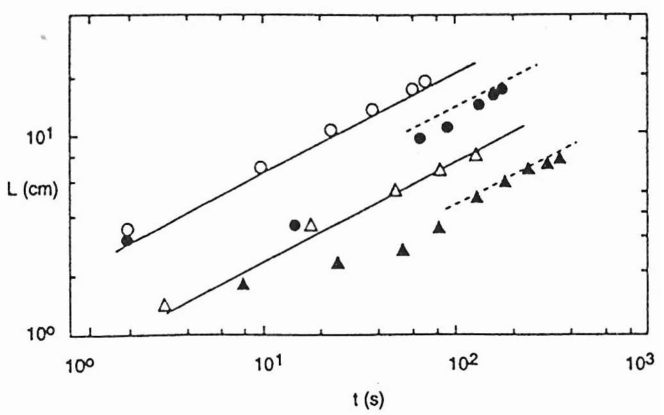


FIG. 4. Measured values of $L$ for different times $t$ for the same four experiments as in Fig. 3. The lines through the experimental data represent the estimate (2) with $\beta(\mathrm{Re})$ given by the graph in Fig. 11 in Ref. 9. The symbols are the same as in Fig. 3.

by the solid lines in graphs in Figs. 3 and 4. As one can see, the measured values of $D$ and $L$ satisfactorily agree with the estimates.

In the second series of the experiments, a cylinder was introduced into the flow. A typical example of the flow evolution in this case is shown in Fig. 5. Initially, the dipole develops freely because the far-field velocities induced by an unsteady dipolar flow decay rapidly with the distance,[2,8] and the cylinder does not influence the flow significantly [see Figs. 1(a) and 5(a)]. When the dipole collides with the cylinder, the interaction begins. At this stage, the secondary dipolar vorticity is intensively generated at the boundary of the cylinder. The primary dipole sweeps the secondary vorticity created at the cylinder boundary and splits into two intermediate dipoles [Figs. 1(b) and 5(b)]. Each newly formed dipole consists of two vortices of opposite sign and of unequal intensity: the secondary vortex being weaker than the primary one. The weaker vortices orbit around the stronger ones and eventually decay [Figs. 1(c) and 5(c)]. As a result of this bifurcation, the remaining primary vortices become weaker. Later, these vortices form a new single dipole [Figs. 1(d) and 5(d)] and finally a newly formed dipole of reduced intensity continues to develop: its size gradually increases while the propagation velocity decreases.

The measured values of $D$ and $L$ for the two experiments with a cylinder are shown by solid symbols in Figs. 3 and 4. Initially, before the collision, the characteristics of the dipole behave in the same manner as the corresponding characteristics of the free dipole. Later, when the interaction begins, the bifurcation occurs and smooth peaks and gaps are clearly seen in the graphs in Figs. 3 and 4. Finally, after the bifurcation, the characteristics of the newly formed dipole demonstrate a different asymptotic behavior compared to that of the free dipole: it moves slower and its width increases faster with distance because the cylinder reduces the momentum of the newly formed dipole.

Using (3) it is possible to calculate the reduction of momentum ($J_0$) of the primary flow by a cylinder and to estimate the reduced intensity $J_*=J-J_0$ of the newly formed dipolar flow. The distribution of the longitudinal velocity in a narrow conical jet, inflowing into a moving dipole, is given by (3). A typical cross-width $\Delta$ of the intense conical flow at the distance $x=\delta$, where the cylinder is placed, is equal to $\Delta=8\delta\nu/\sqrt{J}$. For the values of parameters used in the experiments $\Delta \gg a$, thus the flow running over the cylinder of the radius $a$ is almost uniform in horizontal direction near the axis of the cylinder. A cylinder placed in a flow of amplitude

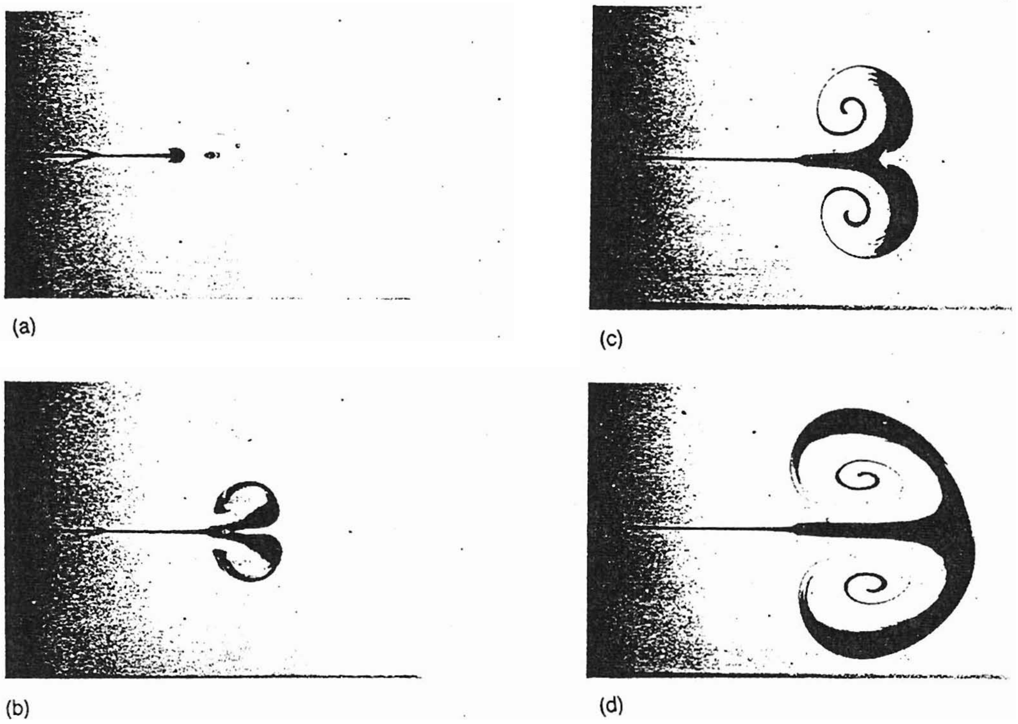


FIG. 5. Sequence of photographs showing the central collision of a planar dipole with a small vertical cylinder. The experimental parameters are $\mathrm{Re}^2=J/\nu^2=4300$; $2a=0.125$ cm; $\delta=3.3$ cm; $N=2\ \mathrm{s}^{-1}$. The photographs were taken at (a) $t=1$, (b) 6, (c) 10, and (d) 31 s after the forcing started.

$V$ acts on the fluid with a drag force $\rho_0 F$. For moderate values of the Reynolds number, $\mathrm{Re}_a = 2aV/\nu$, this force (per unit length of a cylinder) is given by[10]

$$F = \frac{10V^2 a}{\sqrt{\mathrm{Re}_a}}, \tag{4}$$

with accuracy $\simeq 10\%$ for the $\mathrm{Re}_a$ values in the range 0.5–50. To obtain the estimate for the total force, $\rho_0 F_0 = \rho_0 J_0$, applied by the cylinder on the fluid, the distribution (3) must be integrated at $y=0$ over $z$. The integration gives

$$J_0 = \frac{10\sqrt{a\nu}}{\sqrt{2}} \int_{-\infty}^{+\infty} \left( \frac{3\nu \mathrm{Re}}{8\pi\delta[1+(3 \mathrm{Re}\, z^2/64\pi\delta^2)]^2} \right)^{3/2} dz$$

$$= \frac{45}{16} \sqrt{\left(\frac{a}{\delta}\right)} J.$$

Thus the newly formed dipolar flow has the reduced intensity $J_*$ equal to

$$J_* = J - J_0 = J\left[1 - \frac{45}{16}\sqrt{\left(\frac{a}{\delta}\right)}\right]. \tag{5}$$

Using (5) one can calculate the values of $J_*$ and, by means of graphs in Fig. 11 in Ref. 9, estimate the values of $\alpha(\mathrm{Re}_*)$ and $\beta(\mathrm{Re}_*)$ for the reduced nondimensional intensity $\mathrm{Re}_* = \sqrt{J_*}/\nu$ of the newly formed dipolar flow. The dashed lines in Figs. 3 and 4 represent the estimates (1) and (2) with $\alpha$ and $\beta$ obtained by the mentioned procedure.

## IV. MATHEMATICAL MODEL OF THE INTERACTION PROCESS

In the experiments, the primary flow is induced by a localized "point" source of momentum in a stratified fluid. In the vicinity of the source ($x \ll x_0$), the Richardson number defined in Sec. II is small, the buoyancy force does not influence significantly the flow dynamics and the motion is nearly axisymmetric. At $x > x_0$, the buoyancy force prevails. The fluid particles move in horizontal planes and the flow is planar. Because of the viscous friction between horizontal layers, this planar flow is, in fact, three dimensional and the vertical thickness $H$ of the frontal dipole increases with time as[9] $H \propto \sqrt{\nu t}$. Though the total momentum flux transported by the narrow conical jet inflowing into the frontal dipole is constant, the momentum flux per unit thickness of the frontal dipole decreases with time.

In the mathematical model, the fluid is homogenous and the motion is planar and two dimensional at every moment of time. The momentum source, generating the primary flow, is modeled by a line source exerting on the fluid the momentum flux $\rho_0 j$ per unit depth of the fluid, $j$=constant and the dimensions of $j$ are $L^3T^{-2}$.

The basis of the model is the assumption that the action of a small cylinder on the primary flow is similar to the action of another line source of momentum of intensity $j_0$. Thus consider the planar two-dimensional unsteady flow of a viscous homogeneous incompressible fluid induced by two line sources of momentum acting in opposite directions. The fluid is initially at rest and extends to infinity. The first source starts at $t=0$ and thereafter exerts on the fluid a force $\rho_0 j$ per unit depth of the fluid in the direction $\theta=0$ in a polar coordinate system $(r,\theta)$. The second source is at a distance $\delta$ from the first source. It starts at $t=t_0>0$ and exerts on the fluid a force $\rho_0 j_0 (j_0<j)$ in the direction $\theta=\pi$.

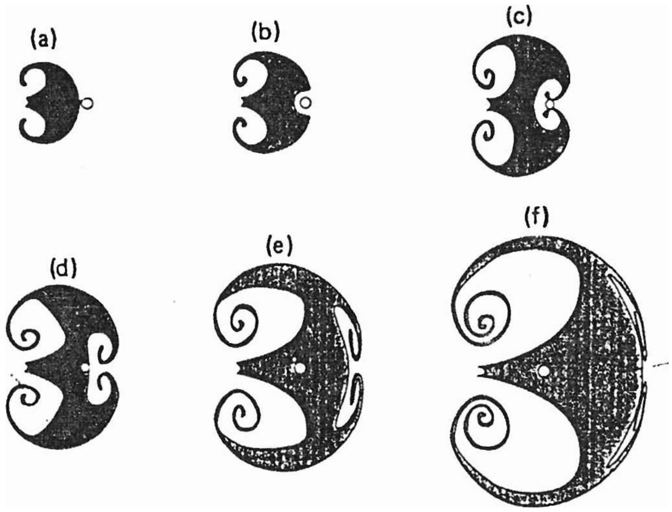


FIG. 6. Dyed water distribution (shaded area) given by the mathematical model for different times. The contours of the shaded area were obtained by the calculations of the trajectories of 172 marked particles. The final positions of the particles for different times were connected by a smooth curve: (a) $t$=1.9, (b) 2.7, (c) 4.2, (d) 5.3, (e) 7.8, and (f) 11.8 s; $j=2j_0$=0.06 cm$^3$ s$^{-2}$, $\nu$=0.01 cm$^2$ s$^{-1}$, $\delta$=0.5 cm.

In the linear approximation, the streamfunction of the considered flow can be presented as the sum of two streamfunctions $\psi_* = \psi + \psi_0$, where $\psi$ describes the primary dipolar flow with the origin at $r=0$ and is given by[2,9]

$$\psi = \frac{jt}{2\pi r}\left(1 - e^{-\eta} - \eta \int_{\infty}^{\eta} \frac{e^{-\zeta}}{\zeta} d\zeta\right) \sin\theta, \quad \eta = \frac{r^2}{4\nu t} \tag{6}$$

The similar expression is used for $\psi_0$, which describes the secondary flow of intensity $j_0$ with the origin at the point $(\delta,0)$.

To "visualize" the flow, the equations of motion

$$\frac{dr}{dt} = r^{-1}\frac{\partial\psi_*}{\partial\theta}, \quad \frac{d\theta}{dt} = -r^{-1}\frac{\partial\psi_*}{\partial r},$$

for marked particles, which the first source emits continuously (as it is in the experiments) are integrated numerically. (In fact. 172 marked particles were emitted from a small circle around the first source.) A typical example of such integration is shown in Fig. 6. In the calculations $j_0=j/2$. The left-hand source generates the primary flow while the right-hand source models the action of a small, two-dimensional body on the flow and is shown by a small circle. The second source starts when the dyed front of the primary dipolar flow reaches the point where it is placed and stops after some period of time.

Comparison of Figs. 5 and 6 demonstrates that in spite of simplicity, the model qualitatively correctly reproduces the main features of the real flow evolution: the formation of the primary dipole at the initial stage [Fig. 6(a)], the splitting of the flow on two intermediate dipoles at the intermediate stage [Figs. 6(c) and 6(d)] and the final formation of a new dipole of reduced intensity at the end of this stage [Figs. 6(e) and 6(f)].

## V. CONCLUSIONS

Summarizing the results presented above, we can conclude that a final result of central collision of a vortex dipole with a small body is a newly formed symmetric dipole of reduced intensity. The reduction of momentum is caused by the nonslip conditions at the boundary of the body and is equal to the drag force of the body. In the case of a small cylinder, this force is calculated and the reduced intensity of a newly formed dipole estimated. It appears that in planar quasi-two-dimensional flows, a dipole is a very stable structure: it survives not only after the collision with another dipole,[9] but also after the collision with a small body. Based on general arguments, one can concluded that symmetry in the interaction is not an essential factor. The symmetric interaction was considered only for the sake of simplicity. Would the cylinder be at the state of rotation or be shifted from the axis of a primary flow, the final result of interaction would be a vortex pair with vortices of different intensities moving in a curved line. To make some quantitative estimates, additional experiments are needed.

## ACKNOWLEDGMENTS

The authors wish to thank I. A. Filippov for technical assistance, P. G. Potylitsin for numerical calculations, and L. A. Mitchell for help in preparing the manuscript. Our thanks are also due to Professor P. Orlandi who stimulated our studies.

[1] M. E. Stern and J. A. Whitehead, "Separation of a boundary jet in a rotating fluid," J. Fluid Mech. **217**, 41 (1990).

[2] S. I. Voropayev and Ya. D. Afanasyev, "Two-dimensional vortex dipole interactions in a stratified fluid," J. Fluid Mech. **236**, 665 (1992).

[3] R. E. Falco, "Coherent motions in the outer region of turbulent boundary layers," Phys. Fluids **20**, 124 (1977).

[4] S. K. Robinson, "Coherent motions in turbulent boundary layer," Annu. Rev. Fluid Mech. **23**, 601 (1991).

[5] G. J. F. van Heijst and J. B. Flor, "Laboratory experiments on dipole structures in a stratified fluid," in *Mesoscale/Synoptic Coherent Structures in Geophysical Turbulence*, edited by J. C. J. Nihoul and B. M. Jamart (Elsevier, Amsterdam, The Netherlands, 1989), p. 591.

[6] P. Orlandi, "Vortex dipole rebound from the wall," Phys. Fluids A **2**, 1429 (1990).

[7] J. Homa, M. Lukas, and D. Rockwell, "Interaction of impulsively generated vortex pairs with bodies," J. Fluid Mech. **197**, 571 (1988).

[8] B. J. Cantwell, "Viscous starting jets," J. Fluid Mech. **173**, 159 (1986).

[9] S. I. Voropayev, Ya. D. Afanasyev, I. A. Filippov, "Horizontal jet and vortex dipoles in a stratified fluid," J. Fluid Mech. **227**, 543 (1991).

[10] G. K. Batchelor, *An Introduction to Fluid Dynamics* (Cambridge University Press, Cambridge, 1967).

[11] S. I. Voropayev and I. A. Neelov, "Laboratory and numerical modeling of vortex dipoles (mushroom-like currents) in a stratified fluid," Okeanologiya **31**, 68 (1991).

[12] S. I. Voropayev and Ya. D. Afanasyev, "Steady horizontal jet in a stratified fluid," Mech. Res. Commun. **18**(6), 435 (1991).